Pergamon

Geochimica et Cosmochimica Acta, Vol. 61, No. 15, pp. 3089–3100, 1997

0016-7037/97 $17.00 + .00

PII S0016-7037(97)00151-8

# New calibration of infrared measurement of dissolved water in rhyolitic glasses

YOUXUE ZHANG[1], R. BELCHER,[1,*] P. D. IHINGER,[2] LIPING WANG,[1] ZHENGJIU XU,[1] and S. NEWMAN[3]

[1]Department of Geological Sciences, The University of Michigan, Ann Arbor, Michigan 48109-1063, USA
[2]Department of Geology and Geophysics, Yale University, New Haven, Connecticut 06520-8109, USA
[3]Division of Geological and Planetary Sciences, California Institute of Technology, Pasadena, California 91125, USA

(*Received December 10, 1996; accepted in revised form April* 1, 1997)

**Abstract**—This paper presents a new calibration for infrared analyses of dissolved water and its species concentrations in rhyolitic glasses. The new calibration combines infrared/manometry measurements and infrared study of hydrous rhyolitic glasses heated at different temperatures. The heating experiments show that the ratio of the molar absorptivity of the 5230 $cm^{-1}$ band to that of the 4520 $cm^{-1}$ band varies with water concentration. Therefore, earlier calibrations assuming constant molar absorptivities are not accurate. Using our new calibration, total water concentration, and species concentrations can be calculated as follows: $(\rho/\rho_0)C_1 = a_0\bar{A}_{523}$, $(\rho/\rho_0)C_2 = (b_0 + b_1\bar{A}_{523} + b_2\bar{A}_{452})\bar{A}_{452}$, and $C = C_1 + C_2$, where $C_1$, $C_2$, and $C$ are the mass fractions of molecular $H_2O$, $H_2O$ present as OH, and total $H_2O$, $\rho/\rho_0$ is the ratio of the density of the hydrous glass to that of the anhydrous glass and is approximately $1 - C$, $\bar{A}_{523}$ and $\bar{A}_{452}$ are the absorbances (peak heights) of the 5230 $cm^{-1}$ and 4520 $cm^{-1}$ bands per mm sample thickness and relative to a baseline that was fit by a flexicurve, $a_0 = 0.04217$ mm, $b_0 = 0.04024$ mm, $b_1 = -0.02011$ $mm^2$, and $b_2 = 0.0522$ $mm^2$. The new calibration has a high internal reproducibility in calculating $H_2O_{total}$, six times better than the calibration of Newman et al. (1986). We expect the new calibration to be accurate in retrieving $H_2O_{total}$ for $H_2O_{total} \leq 5.5$ wt% and in retrieving molecular $H_2O$ and OH concentrations for $H_2O_{total} \leq 2.7$ wt%. Using the new calibration, the equilibrium coefficient $K$ for the reaction $H_2O + O = 2OH$ is independent of $H_2O_{total}$ (for $H_2O_{total} \leq 2.4$ wt%) at a given temperature and can be expressed as $\ln K = 1.876 - 3110/T$, where $T$ is in K. The bulk water diffusivity reported before is not affected by the new calibration, but the molecular $H_2O$ diffusivity will be roughly 4–30% greater. 

## 1. INTRODUCTION

As the most abundant volatile component in terrestrial magmas, dissolved water controls the eruptive power of magma (e.g., Wilson, 1980; Wilson et al., 1980; Woods, 1995; Zhang, 1996; Zhang et al., 1997b) and affects the physical and chemical properties of silicate liquids, such as viscosity (Shaw, 1972; Hess and Dingwell, 1996), density (Lange, 1994; Ochs and Lange, 1997), diffusivity (Watson, 1979), and the crystallization sequence (Wyllie, 1979). Water dissolves into silicate melts as at least two species: $H_2O$ molecules (hereafter referred to as $H_2O_m$) characterized by the infrared (IR) band at 5230 $cm^{-1}$ (1.91 $\mu$m) and OH groups (OH means $X$OH where X ≠ H) characterized by the IR band at 4520 $cm^{-1}$ (2.21 $\mu$m; Fig. 1). The 5230 $cm^{-1}$ band is a combination band due to HOH bending + OH basic stretching, and the 4520 $cm^{-1}$ band due to $X$OH bending/stretching + OH basic stretching. The speciation has been shown to play a significant role in the diffusion of water in silicate liquids and glasses (Zhang et al., 1991a; Zhang and Stolper, 1991), the solubility of water in silicate melts (Blank et al., 1993; McMillan, 1994), and the effect of dissolved water on melt viscosity (Stolper, 1982a). The speciation of water may also affect the fractionation of hydrogen isotopes between silicate melts and water vapor (Newman et al., 1988; Dobson et al., 1989) and the density and thermodynamics of hydrous silicate liquids. The interconversion reaction between the species can be used as a geospeedometer (Zhang et al., 1995, 1997a,b). All the advances in our understanding of the role of water in silicate liquids and glasses require accurate analyses of total water content (hereafter referred to as $H_2O_{total}$) and species concentrations of $H_2O_m$ and OH.

The analytical methods for $H_2O_{total}$ and species concentrations have been summarized by Ihinger et al. (1994). Infrared spectroscopy provides a rapid, nondestructive microbeam technique for quantitative analyses of $H_2O_{total}$ and species concentrations with high precision and sensitivity. It is the only method that is capable of determining $H_2O_{total}$ at low concentrations and determining the $H_2O_m$ and OH species concentrations at present. However, to convert measured IR band intensities into species concentrations requires calibration because of the absence of a good theoretical understanding of the band intensities. The following expressions are used for calibration and for the calculation of species concentrations (Stolper, 1982a; Newman et al., 1986):

$$C = C_1 + C_2 \tag{1a}$$

$$C_1 = \frac{18.015\bar{A}_{523}}{\rho\epsilon_{523}} \tag{1b}$$

$$C_2 = \frac{18.015\bar{A}_{452}}{\rho\epsilon_{452}} \tag{1c}$$

where $C$, $C_1$, and $C_2$ are mass fractions of $H_2O_{total}$, $H_2O_m$,

*Present Address:* Cooper Industry, Abex Friction Products, Winchester, Virginia 22604, USA.

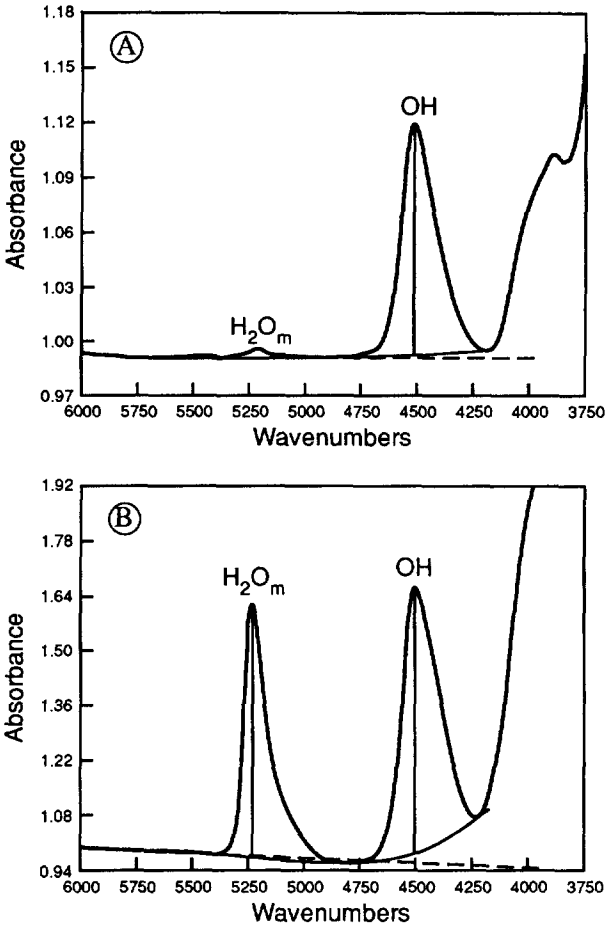


Fig. 1. Infrared spectra of two hydrous glasses, one with 0.172 wt% $H_2O_{total}$ (Fig. 1a) and one with 2.64 wt% $H_2O_{total}$ (Fig. 1b). The 5230 $cm^{-1}$ band is assigned to $H_2O_m$ and the 4520 $cm^{-1}$ band is assigned to OH (Stolper, 1982a). The baseline is fit with a flexicurve and is shown as a solid curve. The straight line fit to the baseline is also shown.

and OH expressed as $H_2O$, $\bar{A}_{5230}$ and $\bar{A}_{4520}$ are absorbances (in terms of peak height) of the 5230 $cm^{-1}$ and 4520 $cm^{-1}$ bands per mm sample thickness, $\rho$ is the density of the glass in g/L (or $kg/m^3$), and $\epsilon_{5230}$ and $\epsilon_{4520}$ are the molar absorptivities for the 5230 $cm^{-1}$ and 4520 $cm^{-1}$ bands in L $mol^{-1}$ $mm^{-1}$. Other bands (including the 3550 $cm^{-1}$ and 7100 $cm^{-1}$ bands, both due to contributions from both $H_2O_m$ and OH) can be calibrated similarly. Stolper (1982a) was the first to calibrate the IR technique for natural and synthetic aluminosilicate glasses but noted the potential error in the known water concentration values for his standard samples. Newman et al. (1986) recalibrated the IR technique using a suite of rhyolitic glasses that were analyzed by manometry and IR, resulting in the widely used molar absorptivities: $\epsilon_{5230} = 0.161$ and $\epsilon_{4520} = 0.173$ L $mol^{-1}$ $mm^{-1}$. Ihinger et al. (1994) noted discrepancies between manometric measurements of water content and IR determination using the Newman et al. (1986) calibration for rhyolitic glasses with high water contents (>2.5 wt%). They reported a revised set of molar absorptivities ($\epsilon_{5230} = 0.186$ and $\epsilon_{4520} = 0.150$ L $mol^{-1}$ $mm^{-1}$) using additional manometry data from Ihinger (1991). In all of these calibrations, each molar absorptivity value for a given anhydrous composition was assumed to be constant, independent of $H_2O_{total}$ and band intensities. Because it has been the most widely used calibration, we concentrate on the calibration of Newman et al. (1986) in subsequent discussions and refer to it as the NSE calibration.

Possible problems with the NSE calibration were indicated by heating experiments. The $H_2O_m$ and OH concentrations for a given $H_2O_{total}$ vary with temperature (e.g., Zhang et al., 1991a; Ihinger et al., 1997; Zhang et al., 1997a; see Fig. 2). One requirement for an accurate calibration is that calculated $H_2O_{total}$ using the calibration should be constant for a piece of glass before and after heating if no water is lost or gained. Skirius et al. (1990) used the IR technique to study water content and speciation in natural and heat-treated/homogenized glass inclusions in quartz. They found that calculated $H_2O_{total}$ using the NSE calibration in similar inclusions after heat treatment is on average 1 wt% (% indicates wt% unless otherwise specified) less than the natural inclusions before heat treatment. They attributed this to an artifact of IR analyses, that is, to the inaccuracy of the NSE calibration. Qin (1994) made similar observations in characterizing the behavior of glass inclusions. In studying water diffusion in rhyolitic glasses, Zhang et al. (1991a) noted that the same piece of glass may have either greater or smaller calculated $H_2O_{total}$ (using the NSE calibration) after heating in air or

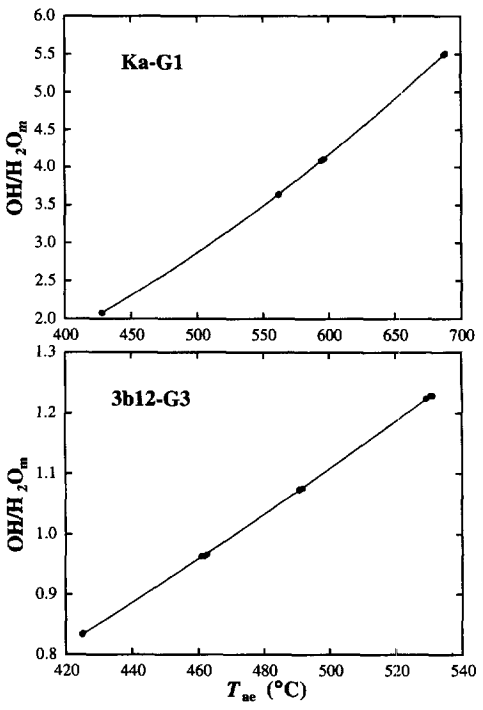


Fig. 2. The variation of $OH/H_2O_m$ ratio (each concentration is in terms of wt% of $H_2O$ calculated using our new calibration) with $T_{ae}$ for two samples (Ka-G1 and 3b12-G3). The curves are simple polynomial fits to guide the eyes.

$N_2$ gas than before heating. They attributed the difference to either the inaccuracy of the NSE calibration or the dependence of molar absorptivities on thermal history. Zhang et al. (1995) noted a similar phenomenon in the study of the kinetics of the interconversion reaction between $H_2O_m$ and OH. Furthermore, using data from their kinetic experiments, Zhang et al. (1995) examined the molar absorptivity ratio ($\epsilon_{523}/\epsilon_{452}$) by rewriting Eqn. 1 as:

$$\bar{A}_{523} = \frac{\rho C}{18.015}\epsilon_{523} - \frac{\epsilon_{523}}{\epsilon_{452}}\bar{A}_{452} \quad (2)$$

They heated the same piece of rhyolitic glass to different equilibrium temperatures ($T_{eq}$) so that $\bar{A}_{523}$ and $\bar{A}_{452}$ vary at constant $\rho C$ (layers affected by significant diffusive loss of $H_2O_{total}$ were polished away before IR analyses). The covariation between $\bar{A}_{523}$ and $A_{452}$ in a series of experiments (all the heating steps and repeated analyses of one point in a wafer constitute a series of experiments) with the same $\rho C$ can be plotted as $\bar{A}_{523}$ vs. $\bar{A}_{452}$ diagram to generate a straight line whose slope is $-\epsilon_{523}/\epsilon_{452}$ if $\epsilon_{523}$ and $\epsilon_{452}$ are constant. They found indeed that good straight lines were obtained and that $\epsilon_{523}/\epsilon_{452} \approx 1.6 \pm 0.3$ based on many series of experiments, in contrast to the ratio of 0.93 (=0.161/0.173) of the NSE calibration. Hence, they concluded that the relative error in the NSE calibration is large. However, since their experiments were carried out to examine the kinetics of the interconversion reaction and were not optimized to determine the molar absorptivity ratios, the $\epsilon_{523}/\epsilon_{452}$ ratio was not constrained sufficiently, and they still used the absorptivities of Newman et al. (1986) for calculating species concentrations. The method used by Zhang et al. (1995) points to a way to constrain the $\epsilon_{523}/\epsilon_{452}$ ratio and hence to calibrate the IR technique. In this paper, we report a new calibration of the molar absorptivities using both manometry constraints and constraints on the $\epsilon_{523}/\epsilon_{452}$ ratio based on heating experiments.

## 2. EXPERIMENTS TO CONSTRAIN THE $\epsilon_{523}/\epsilon_{452}$ RATIO

Heating experiments were carried out in horizontal tube furnaces to constrain the $\epsilon_{523}/\epsilon_{452}$ ratio. The experimental procedures were similar to those of kinetic experiments (Zhang et al., 1995) but were optimized to constrain the $\epsilon_{523}/\epsilon_{452}$ ratio. The optimization was accomplished by varying $\bar{A}_{523}$ and $\bar{A}_{452}$ of the same sample (the same $\rho C$) to the maximum possible extent so that a well-constrained $\bar{A}_{523}$ vs. $\bar{A}_{452}$ plot could be obtained. The variation of $\bar{A}_{523}$ and $\bar{A}_{452}$ was achieved by heating the sample at different temperatures. Two sets of experiments were carried out.

### 2.1. Heating Experiments on Natural Obsidian Glasses

In the first set of experiments, doubly polished wafers of natural obsidian glasses (about $2 \times 3 \times 3$ mm$^3$) were used. The starting glasses were similar to those used in the diffusion, kinetics, and speciation studies (Zhang et al., 1991a, 1995; Ihinger et al., 1997) and are from Mono Craters, California, USA. During the heating experiments, the furnace was first heated to a desired temperature. Each sample was then placed in the furnace and heated. The time for a sample to reach the desired temperature depends on its size and is estimated to be ~10 s. Various temperatures and durations were chosen to maximize the variation in the ratio of the intensities of the two bands (that is, to maximize the range of $T_{ae}$, Zhang, 1994) and to minimize the diffusive loss of water. After heating, the piece was either quenched in liquid nitrogen (with cooling time scale of a few seconds) to preserve the high OH to $H_2O_m$ ratio (because $OH/H_2O_m$ ratio increases with $T_{ae}$), or slowly cooled in air (with cooling time scale of ~1 min) to avoid cracking if a low OH to $H_2O_m$ ratio was desired. Figure 2 shows the variation of $OH/H_2O_m$ ratio with $T_{ae}$ for two samples. Diffusive loss of water was evaluated after each heating step. When the diffusive distance of water, calculated as $(D^*t)^{1/2}$ where $D^*$ is the apparent bulk water diffusivity from Zhang et al. (1991a), was greater than 0.5% of the total thickness of the wafer, the surface layers were polished away to remove the diffusive layers. In this set of experiments, the $H_2O_{total}$ ranges from 0.75% to 2.7%. This $H_2O_{total}$ range is dictated by the following: (1) At $H_2O_{total}$ significantly lower than 0.7%, the relative variation in the 4520 cm$^{-1}$ band would not be enough to produce a well-constrained correlation between $\bar{A}_{523}$ and $\bar{A}_{452}$. (2) There are no large chunks of natural obsidian glass with $H_2O_{total}$ significantly greater than 2.7%. Furthermore, when the $H_2O_{total}$ content is greater than 2.7%, the glass vesiculates easily.

### 2.2. Heating Experiments on Hydrous Rhyolitic Glass Inclusions in Quartz

Because the highest $H_2O_{total}$ is only 2.7% in the first set of experiments, a second set of experiments was carried out using hydrous glass inclusions in quartz crystals from the Bishop Tuff (Skirius et al., 1990). The $H_2O_{total}$ in the glass inclusions is ~5.4%. We chose primary, fresh, and large glass inclusions (120–180 $\mu$m in diameter) that were completely embedded in the crystal, had not devitrified, and had the minimum amount of other inclusions nearby. These inclusion samples were heated to temperatures ranging from 260 to 450°C. Experimental temperatures were kept below 500°C for samples with ~5.4% $H_2O_{total}$ because one sample decrepitated when it was heated to 500°C. (Another inclusion sample with 3.9% $H_2O_{total}$ was used to check the quality of the calibration but not used in the calibration. For this sample, the experimental temperature was kept below 570°C to avoid the $\alpha$-quartz to $\beta$-quartz transition.) After each heating step, the sample was either cooled in air or quenched in liquid $N_2$. Since the experimental temperatures were low, and the inclusions were large, diffusive loss of water through quartz is expected to be negligible. For example, using the treatment of Qin et al. (1992) and with parameters given in Zhang et al. (1991b) and Qin et al. (1992), the loss of water from the inclusions is less than 0.1% relative.

In both sets of experiments, equilibrium $H_2O_m$ and OH concentrations might not be reached in each step at the experimental temperature (that is, $T_{ae}$ may not be the same as $T_{exp}$) because equilibrium is not necessary for our purpose. In order to confirm that the loss of $H_2O_{total}$ is insignificant, the piece might be heated to come back to a $T_{ae}$ that had been reached in a previous heating step to see if the same absorbances were obtained.

### 2.3. Microprobe Analyses

The compositions of the hydrous glasses used in this study were analyzed by electron microprobe at the University of Michigan (Table 1). For inclusions, the analyses were done after the heating experiments by grinding and polishing to reveal the glass inclusion. For bare glasses, the analyses were usually done on the polished and unheated samples. In cases where heated samples were used, a thick layer (ten times thicker than the calculated diffusion distance) was polished away to expose the interior glass that contains the original $H_2O_{total}$. All rhyolitic glasses have similar compositions when normalized on an anhydrous basis (Table 1), as also shown by Newman et al. (1988), Devine et al. (1995), and Hanson et al. (1996). However, there does seem to be a small difference in the anhydrous concentrations of $SiO_2$, $Al_2O_3$, and $Na_2O$ between the bare glasses and inclusion glasses. We assume that the small compositional difference does not significantly affect molar absorptivities.

### 2.4. Infrared Analyses

Each sample was analyzed by Fourier transform infrared spectroscopy (FTIR) before the heating experiments and after each heating

Table 1. Glass composition on an anhydrous basis.*

| Sample | $SiO_2$ | $TiO_2$ | $Al_2O_3$ | FeO | MgO | CaO | $Na_2O$ | $K_2O$ | Sum |
|---|---|---|---|---|---|---|---|---|---|
| Bare glass | | | | | | | | | |
| Ka | 76.68 | 0.01 | 12.66 | 0.94 | 0.01 | 0.51 | 3.95 | 4.83 | 99.59 |
| Mn | 76.67 | 0.05 | 12.61 | 0.96 | 0.03 | 0.54 | 4.12 | 4.78 | 99.75 |
| KS | 76.52 | 0.06 | 12.61 | 1.00 | 0.03 | 0.54 | 4.03 | 4.79 | 99.58 |
| 6b1 | 76.11 | 0.06 | 12.62 | 1.11 | 0.02 | 0.53 | 3.98 | 5.29 | 99.72 |
| POB10 | 76.71 | 0.13 | 12.69 | 0.90 | 0.03 | 0.47 | 3.74 | 4.95 | 99.63 |
| bb3b-11 | 76.99 | 0.12 | 12.64 | 0.97 | 0.03 | 0.54 | 3.95 | 4.81 | 100.05 |
| bb3b-12 | 76.42 | 0.12 | 12.83 | 1.15 | 0.06 | 0.53 | 4.11 | 4.70 | 99.92 |
| Average | 76.59 | 0.08 | 12.67 | 1.00 | 0.03 | 0.52 | 3.98 | 4.88 | 99.75 |
| Inclusion glass | | | | | | | | | |
| 6b-373-3-3-30 | 77.62 | 0.11 | 11.96 | 0.78 | 0.06 | 0.42 | 3.48 | 5.28 | 99.72 |
| LV-81-18A-09 | 78.15 | 0.12 | 12.27 | 0.53 | 0.01 | 0.36 | 3.18 | 5.33 | 99.94 |
| 6b-964 | 77.76 | 0.08 | 12.34 | 0.62 | 0.04 | 0.34 | 3.86 | 4.39 | 99.43 |
| Average | 77.84 | 0.10 | 12.19 | 0.65 | 0.04 | 0.37 | 3.51 | 5.00 | 99.70 |

* Glass analyses were carried out with a Cameca microprobe using a defocused beam (6 $\mu$m in diameter) with 3 nA current. The oxide wt% on an anhydrous basis are calculated by dividing the microprobe measured oxide concentration by $1 - C$ where $C$ is mass fraction of $H_2O_{total}$ (obtained by infrared spectroscopy, see Table 2).

step. For the first set of experiments, because there are small variations in $H_2O_{total}$ even in a single wafer of glass, a chosen point (recognized by microlite bands and other features in the wafer) in the wafer was analyzed three times in each step. That is, we did not analyze three different points in the sample; instead, we analyzed a chosen point three times (with dismounting, cleaning, and remounting the sample to the aperture after each analysis) to gauge and improve the analytical precision. To achieve high precision, effort was made to finish each series of experiments and analyses in a single (long) day so that daily fluctuations of tuning IR instrument can be avoided. This procedure resulted in an average precision of ~0.5% relative. For the more inhomogeneous samples, the maximum difference in the three analyses of the intensity of any band is always less than 2% relative. Vesiculated or cracked areas were no longer used.

For the second set of experiments, initially, an aperture that was smaller than the inclusion was used to analyze a portion of the inclusion, but the reproducibility of the analyses was poor. To improve the reproducibility, an aperture whose diameter (200 $\mu$m or 300 $\mu$m) was greater than the inclusion diameter (120–180 $\mu$m) was used. The large aperture covered not only the whole inclusion, but also part of the quartz crystal. At each step, five repeated analyses of the inclusion were made to improve the precision. Because the aperture covered the inclusion plus some quartz, the spectrum reflects a mixture of inclusion + quartz. Therefore, an IR spectrum of quartz near the inclusion was taken after each heating step, and a fraction of that spectrum is subtracted from each inclusion + quartz spectrum. The fraction equals the volume fraction of quartz over inclusion + quartz covered by the aperture. The error in estimating the fraction does not lead to any noticeable changes in band intensities. All IR analyses on the inclusion and quartz in each series of experiments were along the same orientation of the quartz crystal. The precision on the intensity of each band is better than 2% relative. Because the aperture covered the whole inclusion, which varied in thickness and contained a large amount of quartz, the effective thickness of the glass, and hence the $H_2O_{total}$ could not be estimated. In order to obtain the effective thickness and $H_2O_{total}$, the sample was ground and polished to reveal the glass inclusion on both sides after the heating experiments. The glass (without quartz) was then analyzed using a small aperture. Such an analysis provides information to estimate both the effective thickness and $H_2O_{total}$, though the precision is low (~5%). The inaccuracy in $H_2O_{total}$ and effective thickness does not affect the high accuracy of the $\epsilon_{523}/\epsilon_{452}$ ratio obtained from such experiments.

The baseline of the IR spectrum is fit by a flexicurve and is tangential to the minimum at ~4220 $cm^{-1}$ (Fig. 1). This minimum is clearly not the true baseline and is lifted by the 3950 $cm^{-1}$ band, especially at high $H_2O_{total}$. Therefore, our fitting is precise but not accurate. Other fitting schemes may be chosen to improve the accuracy (such as straight line fits shown in Fig. 1), but the precision would be lower. We chose high precision fitting, because with high precision, a good calibration can compensate for the inaccuracy in the band intensity and yield accurate and precise water concentrations.

## 3. EXPERIMENTAL RESULTS

Twelve series of experiments were conducted using bare obsidian glass and three series of experiments using glass inclusions. All experimental data are reported in Table 2. Results from several series of experiments are plotted as $A_{523}$ vs. $A_{452}$ (Fig. 3). Excellent straight lines are obtained with the slopes giving $-\epsilon_{523}/\epsilon_{452}$ (Eqn. 2). The slopes are obtained from the straight line fit using the algorithm of Albarede and Provost (1977) to account for errors on individual points. We initially hoped that a constant slope (that is, constant $\epsilon_{523}/\epsilon_{452}$) would be obtained, which would make the new calibration relatively simple. While experimental data showed that $\epsilon_{523}/\epsilon_{452}$ depends on $H_2O_{total}$, we then hoped that the variation of $\epsilon_{523}/\epsilon_{452}$ with $H_2O_{total}$ is monotonic. However, experimental data are more complicated.

Figure 3a shows that the slopes for two series of experiments on the same glass wafer are identical within error. Therefore, the results are reproducible. Figure 3b shows that the $\epsilon_{523}/\epsilon_{452}$ ratio first increases from 1.32 at 0.75% $H_2O_{total}$ to 1.7 at 2.7% $H_2O_{total}$, and then decreases to 1.4 at 5.5% $H_2O_{total}$. Two observations can be made: (1) The $\epsilon_{523}/\epsilon_{452}$ ratio is much greater than 0.93 determined by Newman et al. (1986). This is best shown by Fig. 4 in which the calculated $H_2O_{total}$ for several series of experiments is plotted against $T_{ae}$. If the $\epsilon_{523}$ and $\epsilon_{452}$ values of the NSE calibration were accurate, the calculated $H_2O_{total}$ would be constant. However, the calculated $H_2O_{total}$ using the NSE calibration varies smoothly with $T_{ae}$, indicating major revision is necessary for the molar absorptivities. (2) The $\epsilon_{523}/\epsilon_{452}$ ratio is variable

and the variation with $H_2O_{total}$ is not monotonic. It is not clear to us why the $\epsilon_{523}/\epsilon_{452}$ ratio for the two glass inclusions with 5.4–5.5% $H_2O_{total}$ is low (causing the nonmonotonic variation) and whether the low ratio has anything to do with glass inclusions vs. bare glass. However, the low ratio is reproducible for the two inclusions with similar $H_2O_{total}$. Furthermore, we carried out an extra series of experiments using a glass inclusion with 3.9% $H_2O_{total}$ (LV81-18A-09 from a Mono ash flow, Qin, 1994) to check the quality of the calibration. The $\epsilon_{523}/\epsilon_{452}$ ratio for this sample is 1.6, between 1.7 for the bare obsidian glass with 2.7% $H_2O_{total}$ and 1.4 for the inclusions with 5.4% $H_2O_{total}$. Due to a lack of fundamental understanding on how the $\epsilon_{523}/\epsilon_{452}$ ratio should vary, all the variations are viewed to be real and not due to experimental problems. The variation of the $\epsilon_{523}/\epsilon_{452}$ ratio with $H_2O_{total}$ indicates that at least one of the $\epsilon_{523}$ and $\epsilon_{452}$ values is not constant, contrary to the assumption of Newman et al. (1986) that was necessary for them to obtain the $\epsilon_{523}$ and $\epsilon_{452}$ values. Though the nonconstancy of these values is not unreasonable for a major component such as $H_2O$ (e.g., Fine and Stolper, 1985/6 observed that the molar absorptivity for $CO_2$ in synthetic glasses varies for $CO_2$ content greater than 8,000 ppm), the nonconstancy greatly complicates the determination of the molar absorptivities.

In order to check whether the nonconstancy was due to our baseline fitting scheme, we ratioed spectra to a reference spectrum in the same series of experiments. This way, the band at 3950 $cm^{-1}$ is ratioed out, and the baseline near 4220 $cm^{-1}$ is roughly flat. The resulting absorbance is the absorbance difference ($\Delta A$). By plotting $\Delta\bar{A}_{523}$ vs. $\Delta\bar{A}_{452}$, $\epsilon_{523}/\epsilon_{452}$ ratios can be obtained. Although $\epsilon_{523}/\epsilon_{452}$ values obtained this way differ from those obtained in Fig. 3, $\epsilon_{523}/\epsilon_{452}$ values still vary with $H_2O_{total}$ by roughly the same relative amount. Therefore, the variation of $\epsilon_{523}/\epsilon_{452}$ value with $H_2O_{total}$ is real, not an artifact of our fitting procedure that precisely but inaccurately determines the band intensities.

## 4. THE NEW CALIBRATION

The heating experiments discussed above show that a new calibration is necessary. However, the heating experiments can only constrain the $\epsilon_{523}/\epsilon_{452}$ ratio; they cannot provide the complete calibration. In order to obtain a complete calibration, IR measurements and original manometry data from Newman et al. (1986) and Ihinger (1991 and unpubl. data) are combined with the data from heating experiments. We first linearize Eqn. 1 by defining

$$\delta_{523} = \frac{18.015}{\rho_0\epsilon_{523}} \quad \text{and} \quad \delta_{452} = \frac{18.015}{\rho_0\epsilon_{452}} \tag{3}$$

so that

$$\frac{\rho}{\rho_0} C = \delta_{523}\bar{A}_{523} + \delta_{452}\bar{A}_{452} \tag{4}$$

where $\rho_0$ is the density of the anhydrous rhyolitic glass and $\rho$ is the density of the hydrous glass (a function of $C$). The concentration dependence of density can be roughly expressed as $\rho/\rho_0 \approx 1 - C$, obtained by fitting the density vs. mass fraction data of Newman et al. (1986). The uncertainty in the expression of $\rho/\rho_0$ does not significantly affect the calibration. (If the density of hydrous glasses is better constrained in the future, one should still use $\rho/\rho_0 \approx 1 - C$ to calculate species concentrations for internal consistency until a new regression is carried out.)

The concentration dependence of $\delta_{523}$ and $\delta_{452}$ must be specified in order to determine their values. It is expected that at least the molar absorptivity of the 4520 $cm^{-1}$ band should vary with $H_2O_{total}$ (or species concentrations) because of the following: (1) We fit the baseline of the 4520 $cm^{-1}$ band to pass the base at 4220 $cm^{-1}$ for high precision (Fig. 1). Due to the band at 3950 $cm^{-1}$, this fitting procedure increasingly underestimates the 4520 $cm^{-1}$ band intensity, causing an apparent increase in $\delta_{452}$. (2) The OH species can be in the form of AlOH, SiOH, NaOH, etc. (Kohn et al., 1989; Sykes and Kubicki, 1993). As the OH concentration and temperature vary, it is possible that the ratios of these subspecies vary, causing a variation in $\delta_{452}$.

Because the variation of $\epsilon_{523}/\epsilon_{452}$ with $H_2O_{total}$ is not monotonic, as clearly shown by Fig. 3b, a linear dependence of $\delta_{523}$ and $\delta_{452}$ on $H_2O_{total}$ is ruled out. We, therefore, assume a more general dependence of $\delta_{523}$ and $\delta_{452}$: each depends on both $\bar{A}_{523}$ and $\bar{A}_{452}$, used as proxies for $H_2O_m$ and OH. That is, we assumed that $\delta_{523} = a_0 + a_1\bar{A}_{523} + a_2\bar{A}_{452}$, and $\delta_{452} = b_0 + b_1\bar{A}_{523} + b_2\bar{A}_{452}$, where $a_0$, $a_1$, $a_2$, $b_0$, $b_1$, and $b_2$ are fitting parameters. Note that in this formulation, $\delta_{452}/\delta_{523} = \epsilon_{523}/\epsilon_{452}$ would not be constant, but a straight line in $\bar{A}_{523}$ vs. $\bar{A}_{452}$ (Fig. 3) can still result if the variation in the ratio is small for each series of experiments. Each manometry measurement coupled with IR analyses provides one equation for solving these parameters:

$$\bar{A}_{523}a_0 + (\bar{A}_{523})^2a_1 + \bar{A}_{523}\bar{A}_{452}(a_2 + b_1) + \bar{A}_{452}b_0 + (\bar{A}_{452})^2b_2 = \frac{\rho}{\rho_0} C \tag{5}$$

Each series of experimental heating data with constant $(\rho/\rho_0)C$ provides linear constraints for $a_0$, $a_1$, $a_2$, $b_0$, $b_1$, and $b_2$ as:

$$(\bar{A}_{523} - \bar{A}^*_{523})a_0 + [(\bar{A}_{523})^2 - (\bar{A}^*_{523})^2]a_1 + (\bar{A}_{523}\bar{A}_{452} - \bar{A}^*_{523}\bar{A}^*_{452})(a_2 + b_1) + (\bar{A}_{452} - \bar{A}^*_{452})b_0 + [(\bar{A}_{452})^2 - (\bar{A}^*_{452})^2]b_2 = 0 \tag{6}$$

where $\bar{A}_{523}$ represents the average per-mm absorbance for the three (for bare glass wafers) or five (for glass inclusions) repeated analyses of one heating step in a series of experiments, and $\bar{A}^*_{523}$ represents the average absorbance of a reference step in the same series. Note that only $a_2 + b_1$ can be solved; $a_2$ and $b_1$ cannot be separately solved. That is, even the combination of our heating experiments and the manometry data cannot completely constrain how each molar absorptivity varies with species concentrations if we assume each can depend on both $\bar{A}_{523}$ and $\bar{A}_{452}$. The algorithm of Albarede and Provost (1977) was used for the least squares fitting to account for different uncertainties of each point.

The fitting results show that $a_1$ ($0.0002 \pm 0.0023$ $mm^2$, $2\sigma$ error) is indistinguishable from zero, indicating that the

Table 2. Data from heating experiments to constrain the $\varepsilon_{523}/\varepsilon_{452}$ ratio.

| | $T_{exp}$ (°C) | $t$ (s) | $\bar{A}_{523}$ (mm$^{-1}$) | $\bar{A}_{452}$ (mm$^{-1}$) | $T_{ae}$ (°C) |
|---|---|---|---|---|---|
| Piece Ka-G1 (thickness = 3.345 mm; $H_2O_{total}$ = 0.75%) | | | | | |
| Step 0 | Natural | | 0.0572, 0.0577, 0.0574 | 0.1117, 0.1123, 0.1120 | 428 |
| Step 1 | 600 | 240 | 0.0381, 0.0382, 0.0380 | 0.1267, 0.1269, 0.1267 | 562 |
| Step 2 | 750 | 60 | 0.0272, 0.0271, 0.0271 | 0.1346, 0.1348, 0.1348 | 688 |
| Step 3 | 600 | 240 | 0.0346, 0.0347, 0.0346 | 0.1296, 0.1293, 0.1295 | 596 |
| Piece Mnjh-G1 (thickness = 1.282 mm; $H_2O_{total}$ = 0.81%) | | | | | |
| Step 0 | Natural | | 0.0590, 0.0585, 0.0592 | 0.1229, 0.1230, 0.1227 | 459 |
| Step 1 | 600 | 120 | 0.0425, 0.0431, 0.0433 | 0.1349, 0.1342, 0.1346 | 565 |
| Step 2 | 750 | 30 | 0.0312, 0.0307, 0.0310 | 0.1437, 0.1431, 0.1438 | 692 |
| Step 3 | 600 | 120 | 0.0399, 0.0395, 0.0398 | 0.1375, 0.0374, 0.1375 | 595 |
| Piece bb6b1-G1 (thickness = 1.582 mm; $H_2O_{total}$ = 0.97%) | | | | | |
| Step 0 | Natural | | 0.0453, 0.0450, 0.0448 | 0.1597, 0.1602, 0.1607 | 656 |
| Step 1 | 500 | 60 | 0.0511, 0.0508, 0.0511 | 0.1576, 0.1576, 0.1579 | 612 |
| Step 2 | 500 | 180 | 0.0547, 0.0552, 0.0549 | 0.1550, 0.1555, 0.1554 | 584 |
| Step 3 | 500 | 360 | 0.0582, 0.0580, 0.0582 | 0.1527, 0.1523, 0.1526 | 561 |
| Step 4 | 500 | 1,200 | 0.0627, 0.0627, 0.0628 | 0.1487, 0.1489, 0.1489 | 531 |
| Step 5 | 480 | 600 | 0.0640, 0.0635, 0.0635 | 0.1475, 0.1477, 0.1478 | 524 |
| Piece bb6b1-G2 (thickness = 1.862 mm; $H_2O_{total}$ = 1.04%) | | | | | |
| Step 0 | Natural | | 0.0546, 0.0543, 0.0546 | 0.1656, 0.1660, 0.1655 | 624 |
| Step 1 | 500 | 180 | 0.0644, 0.0643, 0.0641 | 0.1606, 0.1610, 0.1603 | 564 |
| Step 2 | 500 | 1200 | 0.0720, 0.0719, 0.0719 | 0.1544, 0.1547, 0.1542 | 519 |
| Step 3 | 710 | 30 | 0.0511, 0.0508, 0.0506 | 0.1693, 0.1693, 0.1697 | 658 |
| Piece bb6b1-G3 (thickness: 1.891 to 1.727 mm due to repolishing; $H_2O_{total}$ = 1.05%) | | | | | |
| Step 0 | Natural | | 0.0559, 0.0563, 0.0563 | 0.1667, 0.1668, 0.1668 | 620 |
| Step 1 | 550 | 180 | 0.0672, 0.0664, 0.0668 | 0.1596, 0.1594, 0.1590 | 551 |
| Step 2 | 470 | 18,000 | 0.0812, 0.0806, 0.0815 | 0.1501, 0.1506, 0.1504 | 482 |
| Step 3 | 550 | 60 | 0.0731, 0.0730, 0.0732 | 0.1562, 0.1558, 0.1565 | 521 |
| Step 4 | 630 | 30 | 0.0547, 0.0552, 0.0552 | 0.1678, 0.1681, 0.1679 | 630 |
| Step 5 | 710 | 20 | 0.0515, 0.0515, 0.0511 | 0.1771, 0.1707, 0.1710 | 661 |
| Piece POB10-G1 (thickness = 2.370 mm; $H_2O_{total}$ = 1.16%) | | | | | |
| Step 0 | Natural | | 0.1037, 0.1038, 0.1042 | 0.1515, 0.1518, 0.1520 | 440 |
| Step 1 | 750 | 20 | 0.0632, 0.0629, 0.0632 | 0.1818, 0.1815, 0.1818 | 643 |
| Step 2 | 600 | 120 | 0.0700, 0.0699, 0.0699 | 0.1768, 0.1763, 0.1765 | 597 |
| Step 3 | 520 | 300 | 0.0826, 0.0821, 0.0821 | 0.1685, 0.1686, 0.1682 | 533 |
| Piece POB10-G2 (thickness = 2.348 mm; $H_2O_{total}$ = 1.18%) | | | | | |
| Step 0 | Natural | | 0.1078, 0.1080, 0.1077 | 0.1533, 0.1533, 0.1538 | 438 |
| Step 1 | 520 | 300 | 0.0945, 0.0945, 0.0944 | 0.1635, 0.1632, 0.1635 | 489 |
| Step 2 | 600 | 120 | 0.0719, 0.0722, 0.0721 | 0.1794, 0.1789, 0.1794 | 598 |
| Step 3 | 750 | 30 | 0.0650, 0.0653, 0.0647 | 0.1841, 0.1844, 0.1832 | 642 |
| Piece bb3b11-G1 (thickness = 2.223 mm; $H_2O_{total}$ = 1.74%) | | | | | |
| Step 0 | Natural | | 0.1447, 0.1449, 0.1445 | 0.2235, 0.2237, 0.2241 | 552 |
| Step 1 | 470 | 600 | 0.1711, 0.1706, 0.1706 | 0.2081, 0.2077, 0.2077 | 478 |
| Step 2 | 570 | 180 | 0.1478, 0.1486, 0.1484 | 0.2196, 0.2200, 0.2204 | 537 |
| Step 3 | 620 | 60 | 0.1368, 0.1366, 0.1362 | 0.2294, 0.2291, 0.2291 | 580 |
| Piece bb3b11-G2 (thickness = 1.925 mm; $H_2O_{total}$ = 1.76%) | | | | | |
| Step 0 | Natural | | 0.1498, 0.1496, 0.1498 | 0.2240, 0.2242, 0.2240 | 544 |
| Step 1 | 470 | 90 | 0.1658, 0.1656, 0.1658 | 0.2159, 0.2163, 0.2163 | 502 |
| Step 2 | 470 | 480 | 0.1748, 0.1743, 0.1741 | 0.2090, 0.2086, 0.2086 | 475 |
| Step 3 | 620 | 120 | 0.1425, 0.1425, 0.1428 | 0.2288, 0.2286, 0.2286 | 567 |
| Piece bb3bHP-G1 (thickness: 0.695 to 0.511 mm due to repeated repolishing; $H_2O_{total}$ = 1.88%) | | | | | |
| Step 1 | From another experiment | | 0.1891, 0.1891, 0.1879 | 0.2207, 0.2207, 0.2207 | 485 |
| Step 2 | 410 | 600 | 0.1963, 0.1960, 0.1957 | 0.2147, 0.2138, 0.2138 | 463 |
| Step 3 | 410 | 18,000 | 0.2147, 0.2152, 0.2147 | 0.2020, 0.2020, 0.2023 | 421 |
| Step 4 | 470 | 300 | 0.1962, 0.1964, 0.1964 | 0.2123, 0.2130, 0.2128 | 460 |
| Step 5 | 540 | 120 | 0.1722, 0.1720, 0.1720 | 0.2297, 0.2295, 0.2297 | 525 |
| Step 6 | 580 | 20 | 0.1557, 0.1565, 0.1546 | 0.2392, 0.2401, 0.2392 | 572 |
| Piece bb3b12-G3 (thickness = 2.346 mm; $H_2O_{total}$ = 2.64%) | | | | | |
| Step 0 | Natural | | 0.309, 0.311, 0.311 | 0.263, 0.264, 0.265 | 462 |
| Step 1 | 420 | 600 | 0.333, 0.332, 0.332 | 0.251, 0.251, 0.251 | 425 |
| Step 2 | 520 | 120 | 0.294, 0.294, 0.293 | 0.273, 0.274, 0.273 | 491 |
| Step 3 | 570 | 60 | 0.274, 0.274, 0.274 | 0.286, 0.286, 0.285 | 530 |

Table 2. (Continued)

| | $T_{exp}$ (°C) | $t$ (s) | $\bar{A}_{523}$ (mm$^{-1}$) | $\bar{A}_{452}$ (mm$^{-1}$) | $T_{ae}$ (°C) |
|---|---|---|---|---|---|
| Piece bb2b12-G3b (thickness = 2.346 mm; $H_2O_{total}$ = 2.68%) | | | | | |
| Step 1 | Same as step 3 above | | 0.279, 0.280, 0.280 | 0.286, 0.288, 02.87 | 528 |
| Step 2 | 420 | 600 | 0.337, 0.336, 0.335 | 0.255, 0.255, 0.255 | 430 |
| Step 3 | 350 | 3,600 | 0.351, 0.351, 0.350 | 0.247, 0.247, 0.248 | 409 |
| Glass inclusion LV-81-18A-09 (effective thickness = 0.063 mm; $H_2O_{total}$ = 3.9%) | | | | | |
| Step 0 | Natural | | 0.705 ± 0.005 | 0.212 ± 0.002 | — |
| Step 1 | 500 | 1,200 | 0.492 ± 0.004 | 0.337 ± 0.002 | — |
| Step 2 | 380 | 40,200 | 0.582 ± 0.003 | 0.298 ± 0.001 | — |
| Step 3 | 440 | 7,200 | 0.531 ± 0.002 | 0.326 ± 0.002 | — |
| Step 4 | 550 | 600 | 0.477 ± 0.002 | 0.357 ± 0.002 | — |
| Glass inclusion 6b-964 (effective thickness = 0.068 mm; $H_2O_{total}$ = 5.4%) | | | | | |
| Step 1 | From other experiments | | 0.987 ± 0.010 | 0.276 ± 0.003 | — |
| Step 2 | 360 | 7,200 | 0.922 ± 0.009 | 0.324 ± 0.004 | — |
| Step 3 | 390 | 3,600 | 0.887 ± 0.008 | 0.342 ± 0.004 | — |
| Step 4 | 420 | 1,800 | 0.866 ± 0.009 | 0.363 ± 0.005 | — |
| Step 5 | 450 | 1,200 | 0.847 ± 0.009 | 0.375 ± 0.005 | — |
| Step 6 | 330 | 14,400 | 0.947 ± 0.006 | 0.306 ± 0.006 | — |
| Step 7 | 260 | 17 days | 1.030 ± 0.009 | 0.252 ± 0.004 | — |
| Glass inclusion 6b-962 (thickness = 0.047 mm; $H_2O_{total}$ = 5.5%*) | | | | | |
| Step 0 | Natural | | 1.076 ± 0.011 | 0.215 ± 0.003 | — |
| Step 1 | 340 | 3,600 | 1.040 ± 0.013 | 0.257 ± 0.002 | — |
| Step 2 | 380 | 1,800 | 0.895 ± 0.009 | 0.338 ± 0.004 | — |
| Step 3 | 420 | 600 | 0.885 ± 0.005 | 0.365 ± 0.002 | — |
| Step 4 | 360 | 3,600 | 0.932 ± 0.014 | 0.325 ± 0.005 | — |
| Step 5 | 450 | 1,200 | 0.850 ± 0.011 | 0.389 ± 0.005 | — |
| Step 6 | 330 | 14,400 | 0.957 ± 0.006 | 0.313 ± 0.004 | — |
| Step 7 | 300 | 57,600 | 0.992 ± 0.010 | 0.286 ± 0.005 | — |

Note: The reported $H_2O_{total}$ are average $H_2O_{total}$ of all steps (with typical $2\sigma$ error or 0.6% relative), calculated using our new calibration. $T_{ae}$ is calculated from Equation (9) of this work. $T_{ae}$ for glass inclusions is not calculated because we do not expect Equation (9) to be accurate at such high $H_2O_{total}$ ($T_{ae}$ for these can be calculated using the speciation model of Ihinger et al., 1997). For bare glasses, the three analyses of band intensities are reported. For inclusions, there are five or more analyses at each step, difficult to put in the table. Hence the average and $2\sigma$ uncertainty at each step are reported.

* This sample was polished too thin after the heating experiments. Thus, direct determination of the thickness and $H_2O_{total}$ was poor and not used. The effective thickness and $H_2O_{total}$ were estimated based on comparison with 6b-964, using band intensity ratios of the sample at different temperatures.

molar absorptivity of the 5230 cm$^{-1}$ band is independent of $H_2O_m$ concentration. Therefore, it may also be independent of OH concentration. Hence, $a_2$ is assumed to be zero. Using the assumptions that $a_1 = 0$ and $a_2 = 0$, the data were refit to give:

$$a_0 = 0.04217 \pm 0.0013 \text{ mm}$$
$$b_0 = 0.04024 \pm 0.0023 \text{ mm}$$
$$b_1 = -0.02011 \pm 0.0051 \text{ mm}^2$$
$$b_2 = 0.0522 \pm 0.0051 \text{ mm}^2 \quad (7)$$

where $2\sigma$ errors are indicated. Therefore, the final formulas for calculating $C$ (mass fraction of $H_2O_{total}$), $C_1$ ($H_2O_m$), and $C_2$ (mass fraction of $H_2O$ present as OH) are:

$$C(1 - C) = a_0\bar{A}_{523} + (b_0 + b_1\bar{A}_{523} + b_2\bar{A}_{452})\bar{A}_{452} \quad (8a)$$
$$C_1 = a_0\bar{A}_{523}/(1 - C) \quad (8b)$$
$$C_2 = (b_0 + b_1\bar{A}_{523} + b_2\bar{A}_{452})\bar{A}_{452}/(1 - C) \quad (8c)$$

From an IR spectrum, the right-hand side of (8a) can be calculated and hence $C$ can be solved from the quadratic equation. $C_1$ and $C_2$ are then obtained from (8b) and (8c).

The variability of $\epsilon_{523}$ and $\epsilon_{452}$ values introduces considerable complexity into the calibration of the IR technique to determine $H_2O_m$ and OH concentrations because one has to specify what factors affect each molar absorptivity and the functional dependence. Since there is no theoretical basis on which such dependence can be predicted, the choice is somewhat arbitrary. It is difficult to evaluate the uncertainties in molar absorptivities introduced by such an arbitrary choice. This difficulty is due to the variability of $\epsilon_{523}$ and $\epsilon_{452}$ values and the lack of direct constraints on the absolute concentration of $H_2O_m$ and OH species. Furthermore, as shown above, it is impossible to solve $a_2$ and $b_1$ separately, and hence impossible to use the above scheme to constrain species concentrations accurately. The assumption that $a_2$ is zero is reasonable but cannot be tested at this time. Therefore, although our new calibration increases the precision and reproducibility in determining $H_2O_{total}$, $H_2O_m$, and OH concentrations, it is difficult to evaluate the accuracy of the calculated $H_2O_m$ and OH concentrations using our new cali-

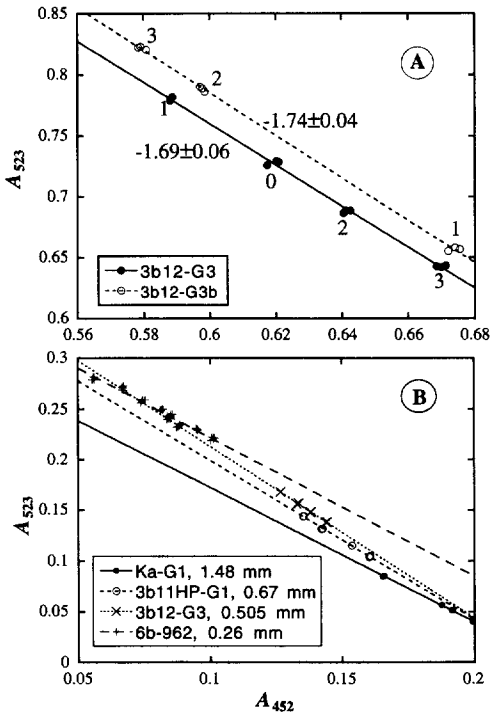


Fig. 3. $A_{523}$ vs. $A_{452}$ diagrams for several series of experiments. (a) $A_{523}$ vs. $A_{452}$ diagram for series bb3b12-G3 (solid dots) and series bb3b12-G3b (open circles). The scatter of the points at each heating step represents uncertainties. The two series represent two different points on the same piece of a sample. The numbers alongside the data points in the figure indicate the heating sequence. 0 means that the piece was natural. After the heating sequence (up temperature and down temperature) of bb3b12-G3, the original point was slightly cracked and another point was chosen in the same piece for the second series of heating steps (bb3b12-G3b). The $H_2O_{total}$ for the second series (bb3b12-G3b) is slightly greater than that for the first series (bb3b12-G3). The thickness of the sample is 2.346 mm. The best fit lines are shown. The slopes of the two series ($-1.69 \pm 0.06$ for series bb3b12-G3 and $-1.74 \pm 0.04$ for series bb3b12-G3b; errors are at the $2\sigma$ level) are indistinguishable. (b) $A_{523}$ vs. $A_{452}$ diagram for four series with different $H_2O_{total}$ (Ka-G1, 0.75%; bb3b11HP-G1, 1.88%; bb3b12-G3, 2.64%; inclusion 6b-962, 5.5%). The absorbances of each wafer are normalized to a thickness given in the figure so that the absorbances for the four wafers can be conveniently plotted on a single diagram and can be compared. The slopes for the four samples are clearly different, indicating different $\epsilon_{523}/\epsilon_{452}$ ratio ($1.32 \pm 0.03$ for series Ka-G1, $1.57 \pm 0.05$ for bb3b11HP-G1, $1.69 \pm 0.06$ for bb3b12-G3, and $1.37 \pm 0.07$ for 6b-962).

bration, especially at high $H_2O_{total}$ where the constraints are fewer. Our new calibration results in constant equilibrium coefficient for the reaction $H_2O_m + O = 2OH$ at a given temperature (see later discussion), which is considered to be strong evidence indicating that our new calibration is accurate at $H_2O_{total} < 2.7\%$.

The extra series of experiments (LV81-18A-09) was carried out to confirm the reproducibility of $H_2O_{total}$. The inclusion contains 3.9% $H_2O_{total}$ that lies between the highest $H_2O_{total}$ in bare glasses (2.7%) and $H_2O_{total}$ in the glass inclusions used in the calibration (5.4%). The experiments were carried out after the above calibration was obtained and were not used in the regression in obtaining $a_0$, $b_0$, $b_1$, and $b_2$. Instead, the experiments were used to check the accuracy of the calibration. Calculated $H_2O_{total}$ using our new calibration and that of NSE as a function of $T_{ae}$ is shown in the last figure of Fig. 4. The constancy of $H_2O_{total}$ calculated using our new calibration confirms our calibration.

## 5. DISCUSSION

### 5.1. Comparison with Previous Results

The new calibration is compared below with the calibration of Newman et al. (1986) in terms of (1) accuracy in $H_2O_{total}$ (comparison between calculated $H_2O_{total}$ and manometry data), (2) reproducibility in $H_2O_{total}$ (whether $H_2O_{total}$ calculated for a series of heating experiments is constant), and (3) accuracy and precision in calculated species concentrations. In this work, reproducibility is defined to be different from precision: Precision is the repeatability of both $H_2O_m$ and OH concentrations by analyzing the same point without any new heat treatment, whereas reproducibility is defined as the repeatability of $H_2O_{total}$ concentration by analyzing the same point with repeated heat treatments and hence with changing species concentrations. Accuracy is the ability to obtain the actual concentrations of $H_2O_{total}$, $H_2O_m$, and OH.

(1) Accuracy in the calculated $H_2O_{total}$. The calibration of Newman et al. (1986) can reproduce very well not only the manometry $H_2O_{total}$ data by Newman et al. (1986), but also the new manometry data by Ihinger (1991 and unpubl. data). In terms of the manometry data alone, our new calibration (Fig. 5) improves the NSE calibration only slightly ($\chi^2$ of our new calibration is 15% smaller than that of the NSE calibration). There is a significant difference in calculated $H_2O_{total}$ between our new calibration and the NSE calibration at high $H_2O_{total}$. For example, for 6b-962, the $H_2O_{total}$ is 5.5% using our new calibration but 5.9–6.3% using the NSE calibration. The NSE calibration used only hydrous glasses with $H_2O_{total} < 2.0\%$ and the inaccuracy at high $H_2O_{total}$ is not surprising. The results show that (a) further improvement of our calibration requires improving the accuracy of manometry data; (b) the NSE calibration is good in terms of calculating $H_2O_{total}$ content; and (c) it is almost impossible to constrain the molar absorptivities using manometry data alone given the present accuracy of manometry measurements if the molar absorptivities vary as a function of species concentrations.

(2) Reproducibility in obtaining constant $H_2O_{total}$ for a series of heating experiments. As shown in Fig. 4, $H_2O_{total}$ calculated using the NSE calibration for a series of heating experiments with constant $H_2O_{total}$ shows systematic variation with $T_{ae}$, whereas our new calibration reproduces the constant $H_2O_{total}$ in the series of heating experiments. In terms of internal consistency to reproduce constant $H_2O_{total}$, our new calibration improves that of the NSE calibration by almost an order of magnitude (the $2\sigma$ relative precision is 0.7% for the new calibration vs. 4% for the NSE calibration).

The effect of our new calibration on analytical uncertainties can be clarified using the following example. Two glasses (A and B) are analyzed by FTIR for $H_2O_{total}$. Ini-

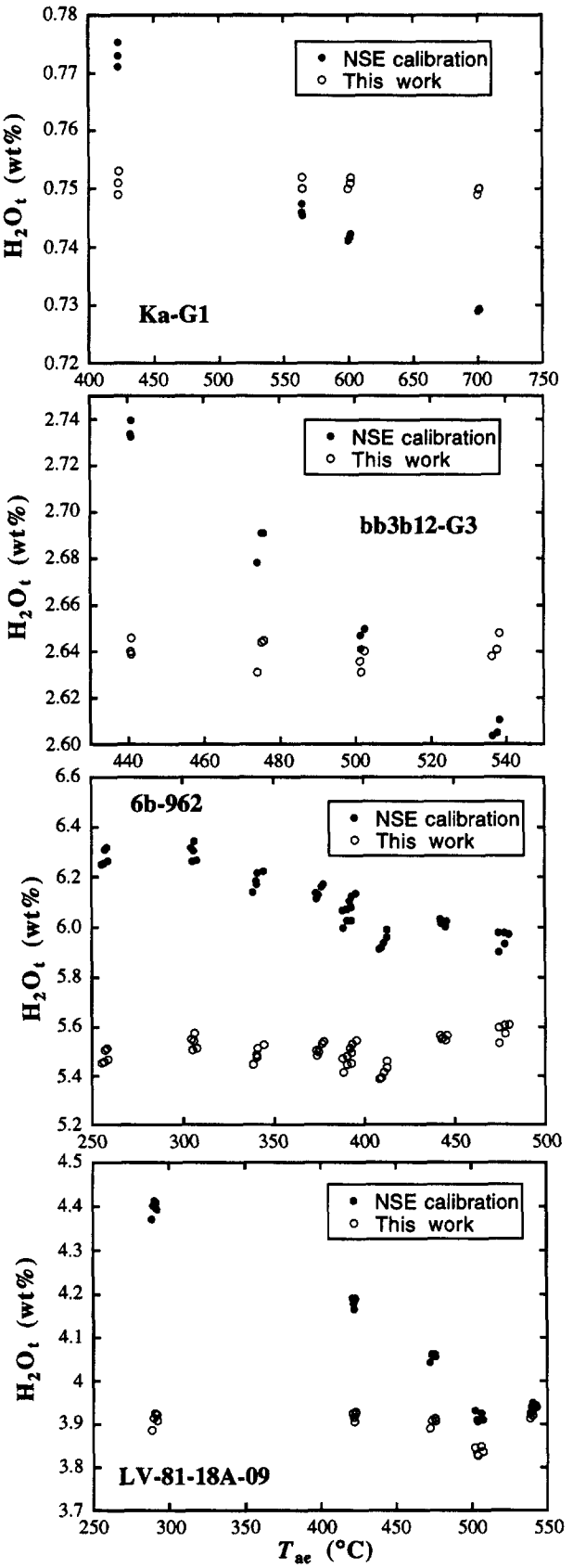


tially, we use the old NSE calibration. Next we use the new calibration. In both cases the results reveal nominal $H_2O_{total}$ of 3.10% for A and 3.20% for B. The imprecision associated with the NSE calibration allows the possibility that A and B have the same $H_2O_{total}$ (3.3–2.9% for A) and (3.4–3.0% for B). However, for the new calibration $H_2O_{total}$ in B is always about 0.1% greater than in A, although the absolute concentrations in both A and B still have about the same uncertainty.

(3) Accuracy and precision in calculated species concentrations. The molecular $H_2O$ concentration using our calibration is 10% less than that using the NSE calibration. At low $H_2O_{total}$, the OH concentration determined using our calibration is within 10% of that obtained using the NSE calibration. At higher $H_2O_{total}$ (>2.7%), the difference between OH calculated using our new calibration and that using the NSE calibration can be large (approaching 45% relative difference) or small, depending on the ratio of the two bands. Because the reproducibility in calculated $H_2O_{total}$ using our new calibration is much better than that of the NSE calibration, we infer that the precision in calculated species concentrations using our calibration is also better. However, it is difficult to evaluate the accuracy of the calculated $H_2O_m$ and OH concentrations as discussed above.

The calibration of Ihinger et al. (1994) is closer to our new calibration than the calibration of Newman et al. (1986). However, because Ihinger et al. (1994) assumed that $\epsilon_{523}$ and $\epsilon_{452}$ values were constant, their calibration is not consistent with our experimental heating data and our new calibration.

### 5.2. Water Speciation Model

Our new calibration has been adopted by Ihinger et al. (1997) in their study of the dependence of hydrous species concentrations on temperature in rhyolitic melts. Using the NSE calibration, the equilibrium coefficient $K$ ($=[OH]^2/\{[H_2O_m][O]\}$) decreases with increasing $H_2O_{total}$ (Zhang et al., 1991a, 1995). Thus, if the NSE calibration indeed re-

Fig. 4. $H_2O_{total}$ vs. $T_{ae}$ for three series of heating experiments. $T_{ae}$ is calculated from $T_{ae} = (2660 + 89.6\,\bar{A}_{523} + 1082\,\bar{A}_{452})/(2.482 - \ln(\bar{A}^2_{452}/\bar{A}_{523})) - 273.15$ (Ihinger et al., 1997). Equation 9 is not used because it does not provide an accurate description of $K$ for high $H_2O_{total}$ samples either due to nonideal mixing at the high $H_2O_{total}$ or due to the inaccuracy in $H_2O_m$ and OH contents using our new calibration for high $H_2O_{total}$ samples. Hence $T_{ae}$ values in this figure may be slightly (up to 15°C) different from those in Table 2. $H_2O_{total}$ is calculated using our new calibration (open circles) and using that of NSE (dots). $H_2O_{total}$ should be constant (that is, the points should form a roughly horizontal line in each graph). Clearly, calculated $H_2O_{total}$ using the NSE calibration is variable, which implies that the NSE calibration is not accurate. The calculated $H_2O_{total}$ using our new calibration typically varies by 0.6% relative for any series of heating experiments, approaching the precision in determining IR band intensities. The four experimental series are Ka-G1 (the best reproducibility using our new calibration), bb3b12-G3, 6b-962 (the worst reproducibility using our new calibration, but still very good), and LV-81-18A-09. Data for the fourth series (LV-81-18A-09) were not used in obtaining the new calibration but were used to provide an independent check of the calibration.

turned the true species concentrations, the mixing of the three oxygen species in hydrous rhyolite would be nonideal, and higher order mixing models would be required to describe the interaction of the oxygen species in silicate melt (e.g., Ihinger, 1991; Zhang et al., 1991a). However, using our new calibration and the original IR data of Zhang et al. (1991a, 1995), the calculated equilibrium coefficient depends only on temperature and is independent of $H_2O_{total}$ for $H_2O_{total}$ from 0.5% to 2.4% (Fig. 6). That is, our derived molar absorptivities, based on a completely independent dataset, return species concentrations demonstrating that the simplest possible interactions occur between the three oxygen species (i.e., no interaction parameters are required to model the data). Thus, at least for samples with $H_2O_{total} \leq 2.4\%$, mixing of hydrous species in rhyolitic melt is ideal. This simple result lends strong support that our new calibration accurately reflects the species concentrations in rhyolitic glass. The dependence of $\ln K$ on temperature can now be simply expressed as (Fig. 6b):

$$\ln K = 1.876 - 3110/T \qquad (9)$$

with the enthalpy of the reaction being 25.9 ± 0.6 kJ. This $\Delta H$ of the reaction is similar to that of Dingwell and Webb (1990) and Zhang et al. (1991a). Because the calibration is best constrained at $H_2O_{total} < 2.7\%$, and all experimental speciation data were for $H_2O_{total} < 2.4\%$ (all data by Zhang et al., 1991a, 1995), Eqn. 9 should not be used for $H_2O_{total} > 2.7\%$.

Use of any speciation model to calculate $T_{ae}$ depends primarily on the absorbances and is independent of the molar absorptivities as long as the same absorptivities are used both in the calibration of the model and in the calculation of $T_{ae}$ of a sample (that is, as long as there is internal consistency). Therefore, calculating $T_{ae}$ using the formula in Zhang et al. (1991a) is still accurate as long as one uses the NSE calibration to calculate the species concentrations. $T_{ae}$ can also be calculated simply from $\bar{A}_{523}$ and $\bar{A}_{542}$ (Ihinger et al., 1997), without knowing the actual species concentrations.

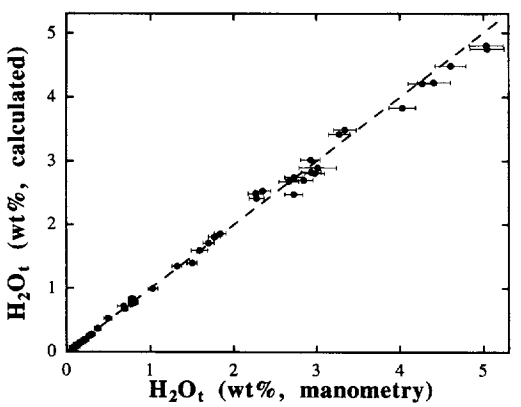


Fig. 5. Comparison of calculated and measured $H_2O_{total}$ (manometry data with $2\sigma$ error bars). The line is a 1:1 line. Manometry data are from Newman et al. (1986) and Ihinger (1991 and unpubl. data). The error assignment of data from Ihinger (1991 and unpubl. data) is based on the larger of (1) the uncertainty associated with the manometric technique dependent on sample size, and (2) 2% relative error. The error assignment for manometry data of Newman et al. (1986) is the greater of (1) the error assigned in Newman et al. (their Table 1), (2) 0.02 wt% $H_2O_{total}$ (reflecting the difficulty to extract OH at very low $H_2O_{total}$), and (3) 2% relative error.

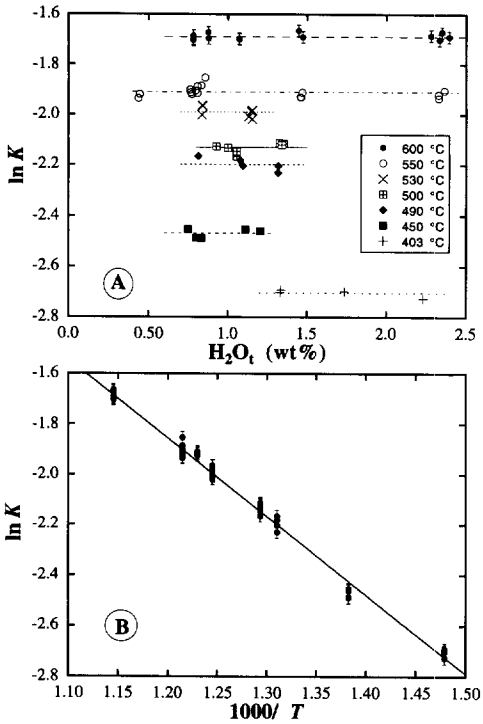


Fig. 6. Equilibrium coefficient $K$ ($=[OH]^2/\{[H_2O_m][O]\}$) in quenched rhyolitic glasses. The experimental temperature ranges from 400 to 600°C. Data are from Zhang et al. (1991a) and Zhang et al. (1995). (a) $\ln K$ as a function of $H_2O_{total}$. Error bars for 600°C data are indicated. Error bars for other data are similar but not shown for clarity. At each temperature, $K$ is constant within error. (b) $\ln K$ as a function of temperature. The solid line is a best-fit line.

### 5.3. Apparent Bulk Water Diffusivity and Molecular $H_2O$ Diffusivity

Zhang et al. (1991a) in their diffusion study calculated $H_2O_m$ and OH concentrations from IR spectra using the NSE calibration. Therefore, $H_2O_m$ concentration and $d[H_2O_m]/d[H_2O_{total}]$ were systematically underestimated. Of interests is the accuracy or inaccuracy of the apparent bulk water diffusivities and molecular $H_2O$ diffusivities reported by Zhang et al. (1991a). Since the apparent bulk water diffusivity calculated using the data and formulation of Zhang et al. (1991a) is independent of estimated $H_2O_m$ concentrations, calculated apparent bulk water diffusivity will be correct in the $H_2O_{total}$ range of the experiments ($\leq 1.8\%$ $H_2O_{total}$, Zhang et al., 1991a; and one datum from Wang et al., 1996). However, caution should be exercised in extrapolating the model to calculate apparent bulk water diffusivity to greater $H_2O_{total}$.

The calculated $H_2O_m$ diffusivity depends on the calculated species concentrations. Therefore, using our new calibration

and new speciation model above, $H_2O_m$ diffusivities are roughly 4–30% greater than those reported in Zhang et al. (1991a), depending on $H_2O_{total}$ and temperature. For example, for sample KS-D3 at 490°C in Zhang et al. (1991a), the $H_2O_m$ diffusivity calculated using the new calibration is 0.043 $\mu m^2/s$ instead of the reported 0.040 $\mu m^2/s$.

### 5.4. Other Hydrous Silicate Glasses

On the basis of our results, assuming constant molar absorptivities for albitic and other glasses is likely only appropriate to a first order accuracy. Manometry constraints alone may not be able to resolve the variability of the molar absorptivities of the hydrous species in these glasses. Accurate determination of water and hydrous species concentrations in these glasses requires manometry constraints together with constraints from heating experiments.

## 6. CONCLUSIONS

Our new calibration greatly improves the precision and reproducibility of calculated $H_2O_{total}$ over the NSE calibration. Besides producing constant $H_2O_{total}$ for a sample heated to different temperatures, the new calibration also results in an $H_2O_{total}$-independent $K$ for $H_2O_{total} \leq 2.4\%$ for reaction $H_2O_m + O = 2OH$ at a given temperature. The calculation of apparent bulk water diffusivity as a function of $H_2O_{total}$ is independent of calibration of species concentrations. However, the molecular $H_2O$ diffusivity depends on the measurement of species concentrations. Using our new calibration, the calculated molecular $H_2O$ diffusivity is slightly greater than that reported in Zhang et al. (1991a).

Our own assessment of the new calibration is that (1) the new calibration is accurate in calculating $H_2O_{total}$ and (2) the new calibration is reliable for calculating species concentrations for $H_2O_{total} \leq 2.7\%$ since most of the experimental heating data are in this $H_2O_{total}$ range. Almost all obsidian glasses in pyroclastic deposits have $H_2O_{total}$ less than 2.7%. Hence our new calibration can be applied widely. At greater $H_2O_{total}$ (for glass inclusions), our new calibration is reliable in retrieving $H_2O_{total}$, but may not be very reliable in terms of species concentrations. We encourage future authors to include the original IR band intensities ($\bar{A}_{523}$ and $\bar{A}_{452}$) in reporting $H_2O_m$ and OH concentrations.

*Acknowledgments*—Glass inclusions in quartz phenocrysts from the Bishop Tuff and Mono ash flows were prepared and provided by A. T. Anderson with help from Nathaniel Brown. We greatly appreciate their generous help. We thank A. T. Anderson and P. F. McMillan for constructive comments. This work was supported by NSF grants EAR-9315918 and EAR-9458368.

## REFERENCES

Albarede F. and Provost A. (1977) Petrological and geochemical mass-balance equations: an algorithm for least-square fitting and general error analysis. *Comput. Geosci.* **3,** 309–326.

Blank J. G., Stolper E. M., and Carroll M. R. (1993) Solubilities of carbon dioxide and water in rhyolitic melt at 850°C and 750 bars. *Earth Planet. Sci. Lett.* **119,** 27–36.

Devine J. D., Gardner J. E., Brack H. P., Layne G. D., and Rutherford M. J. (1995) Comparison of microanalytical methods for estimating $H_2O$ contents of silicic volcanic glasses. *Amer. Mineral.* **80,** 319–328.

Dingwell D. B. and Webb S. L. (1990) Relaxation in silicate melts. *Eur. J. Mineral.* **2,** 427–449.

Dobson P. F., Epstein S., and Stolper E. M. (1989) Hydrogen isotope fractionation between coexisting vapor and silicate glasses and melts at low pressure. *Geochim. Cosmochim. Acta* **53,** 2723–2730.

Fine G. and Stolper E. M. (1985/86) Dissolved carbon dioxide in basaltic glasses: concentrations and speciation. *Earth Planet. Sci. Lett.* **76,** 263–278.

Hanson B., Delano J. W., and Lindstrom D. J. (1996) High-precision analysis of hydrous rhyolitic glass inclusions in quartz phenocrysts using the electron microprobe and INAA. *Amer. Mineral.* **81,** 1249–1262.

Hess K. and Dingwell D. B. (1996) Viscosities of hydrous leucogranitic melts: A non-Arrhenian model. *Amer. Mineral.* **81,** 1297–1300.

Ihinger P. D. (1991) An experimental study of the interaction of water with granitic melt. Ph.D., California Inst. Tech.

Ihinger P. D., Hervig R. L., and McMillan P. F. (1994) Analytical methods for volatiles in glasses. *Rev. Mineral.* **30,** 67–121.

Ihinger P. D., Zhang Y., and Stolper E. M. (1997) The speciation of dissolved water in rhyolitic melt. *Geochim. Cosmochim. Acta* (submitted).

Kohn S. C., Dupree R., and Smith M. E. (1989) A multinuclear magnetic resonance study of the structure of hydrous albite glasses. *Geochim. Cosmochim. Acta* **53,** 2925–2935.

Lange R. A. (1994) The effect of $H_2O$, $CO_2$, and F on the density and viscosity of silicate melts. *Rev. Mineral.* **30,** 331–369.

McMillan P. F. (1994) Water solubility and speciation models. *Rev. Mineral.* **30,** 131–156.

Newman S., Stolper E. M., and Epstein S. (1986) Measurement of water in rhyolitic glasses: Calibration of an infrared spectroscopic technique. *Amer. Mineral.* **71,** 1527–1541.

Newman S., Epstein S., and Stolper E. M. (1988) Water, carbon dioxide, and hydrogen isotopes in glasses from the ca. 1340 A.D. eruption of the Mono Craters, California: Constraints on degassing phenomena and initial volatile content. *J. Volcanol. Geotherm. Res.* **35,** 75–96.

Ochs F. A. and Lange R. A. (1997) The partial molar volume, thermal expansivity, and compressibility of $H_2O$ in $NaAlSi_3O_8$ liquid: New measurements and an internally consistent model. *Contrib. Mineral. Petrol.* (in press).

Qin Z. (1994) I. Diffusive reequilibration of melt inclusions. II. Mathematical modeling of chemical fractionation during mantle melting. Ph.D., Univ. Chicago.

Qin Z., Lu F., and Anderson A. T. (1992) Diffusive reequilibration of melt and fluid inclusions. *Amer. Mineral.* **77,** 565–576.

Shaw H. R. (1972) Viscosities of magmatic silicate liquids: An empirical method of prediction. *Amer. J. Sci.* **272,** 870–893.

Skirius C. M., Peterson J. W., and Anderson J. (1990) Homogenizing rhyolitic glass inclusions from the Bishop Tuff. *Amer. Mineral.* **75,** 1381–1398.

Stolper E. M. (1982a) Water in silicate glasses: An infrared spectroscopic study. *Contrib. Mineral. Petrol.* **81,** 1–17.

Stolper E. M. (1982b) The speciation of water in silicate melts. *Geochim. Cosmochim. Acta* **46,** 2609–2620.

Sykes D. and Kubicki J. D. (1993) A model for $H_2O$ solubility mechanisms in albite melts from infrared spectroscopy and molecular orbital calculations. *Geochim. Cosmochim. Acta* **57,** 1039–1052.

Wang L., Zhang Y., and Essene E. J. (1996) Diffusion of the hydrous component in pyrope. *Amer. Mineral.* **81,** 706–718.

Watson E. B. (1979) Diffusion of cesium ions in $H_2O$-saturated granitic melt. *Science* **205,** 1259–1260.

Wilson L. (1980) Relationships between pressure, volatile content, and ejecta velocity in three types of volcanic explosions. *J. Volcanol. Geotherm. Res.* **8,** 297–313.

Wilson L., Sparks R. S. J., and Walker G. P. L. (1980) Explosive volcanic eruptions—IV. The control of magma properties and conduit geometry on eruption column behavior. *Geophys. J. Roy. Astro. Soc.* **63,** 117–148.

Woods A. W. (1995) The dynamics of explosive volcanic eruptions. *Rev. Geophys.* **33,** 495–530.

Wyllie P. J. (1979) Magmas and volatile components. *Amer. Mineral.* **64,** 469–500.

Zhang Y. (1994) Reaction kinetics, geospeedometry, and relaxation theory. *Earth Planet. Sci. Lett.* **122,** 373–391.

Zhang Y. (1996) Dynamics of $CO_2$-driven lake eruptions. *Nature* **379,** 57–59.

Zhang Y. and Stolper E. M. (1991) Water diffusion in basaltic melts. *Nature* **351,** 306–309.

Zhang Y., Stolper E. M., and Wasserburg G. J. (1991a) Diffusion of water in rhyolitic glasses. *Geochim. Cosmochim. Acta* **55,** 441–456.

Zhang Y., Stolper E. M., and Wasserburg G. J. (1991b) Diffusion of a multi-species component and its role in the diffusion of water and oxygen in silicates. *Earth Planet. Sci. Lett.* **103,** 228–240.

Zhang Y., Stolper E. M., and Ihinger P. D. (1995) Kinetics of reaction $H_2O + O = 2OH$ in rhyolitic glasses: Preliminary results. *Amer. Mineral.* **80,** 593–612.

Zhang Y., Jenkins J., and Xu Z. (1997a) Kinetics of the reaction $H_2O + O = 2OH$ in rhyolitic glasses upon cooling: geospeedometry and comparison with glass transition. *Geochim Cosmochim Acta* **61,** 2167–2173.

Zhang Y., Sturtevant B., and Stolper E. M. (1997b) Dynamics of gas-driven eruptions: Experimental simulations using $CO_2$-$H_2O$-polymer system. *J. Geophys. Res.* **102,** 3077–3096.